

THE DEVELOPMENT OF HIGH ORDER NUMERICAL TECHNIQUES FOR  
REENTRY SIMULATION OF HYPERSONIC SPACECRAFT

Final Report

NASA/ASEE Summer Faculty Fellowship Program – 1991

Johnson Space Center

Prepared By:	Richard Sanders
Academic Rank:	Associate Professor
University and Dept.:	University of Houston - University Park Department of Mathematics Houston, Texas 77204-3476

NASA/JSC

Directorate:	Engineering and Development
Division:	Navigation, Control and Aeronautics Division
Branch:	Aeroscience Branch
JSC Colleague:	Chin Li
Date Submitted:	November 15, 1991
Contract Number:	NGT 44-001-800

**Abstract.** The primary difficulty encountered when simulating hypersonic flow is the flow normally includes strong nonlinear discontinuities. These discontinuities fall into three broad classes: shocks, slip-lines and rarefaction waves. Moreover, in the hypersonic flow regime, the chemistry of hot gases plays a vital role and can not be neglected. These facts combine to make the numerical treatment of spacecraft reentry a most challenging problem. In this work, we develop a class of finite difference schemes that accurately resolve discontinuous solutions to spacecraft reentry flow and are simple to incorporate into existing spacecraft reentry codes.

**§1. Introduction.** The most simple finite difference schemes for the numerical approximation of partial differential equations are easy to motivate. Basically what one does is replace derivatives by finite difference quotients that approximate them. However, this recipe does not always guarantee a stable scheme. To see this, consider the pde:

$$(1.1) \quad \begin{aligned} \frac{\partial u}{\partial t} + \lambda \frac{\partial u}{\partial x} &= 0 \\ u(x, 0) &= u_0(x). \end{aligned}$$

Let  $t^n$  denote  $n\Delta t$  with  $n = 0, 1, 2, \dots$  and  $x_j$  denote  $j\Delta x$  with  $j = \dots, -1, 0, 1, \dots$ . Let the grid function  $u_j^n$  approximate  $u(x_j, t^n)$ . One possible finite difference scheme to approximate the solution to the pde above is:

$$\begin{aligned} \text{Replace } \frac{\partial u}{\partial t} &\text{ with } \frac{u_j^{n+1} - u_j^n}{\Delta t}. \\ \text{Replace } \frac{\partial u}{\partial x} &\text{ with } \frac{u_{j+1}^n - u_{j-1}^n}{2\Delta x}. \end{aligned}$$

This gives an explicit time marching scheme

$$u_j^{n+1} = u_j^n - \frac{\Delta t}{2\Delta x} \lambda (u_{j+1}^n - u_{j-1}^n).$$

Applying this scheme to discrete initial data

$$u_j^0 = e^{i\theta x_j},$$

we obtain an exact solution

$$\begin{aligned} u_j^n &= (g(\theta\Delta x))^n e^{i\theta x_j} \\ g(\theta) &= 1 - \frac{\Delta t}{\Delta x} \lambda i \sin(\theta). \end{aligned}$$

$g(\theta)$  is called the amplification factor. For all  $\pi > |\theta| > 0$  we have that  $|g(\theta)| > 1$ . Therefore, the amplitude of every wave component with  $\pi > |\theta\Delta x| > 0$  blows up geometrically – this scheme is unstable.

A desirable feature of the scheme above is the centered difference approximation for  $\partial/\partial x$ . In addition to its second order accuracy, central space differencing schemes require only a three point stencil. There are ways to construct *linearly stable* central space differencing finite difference schemes to solve (1.1). For example,

$$\begin{aligned} \text{Replace } \frac{\partial u}{\partial t} & \text{ with } \frac{u_j^{n+1} - u_j^n}{\Delta t}. \\ \text{Replace } \frac{\partial u}{\partial x} & \text{ with } \frac{u_{j+1}^{n+1} - u_{j-1}^{n+1}}{2\Delta x}, \end{aligned}$$

defines what is called backward Euler time discretization. This implicit scheme is unconditionally stable. Another implicit scheme that is unconditionally stable is the trapezoidal rule. It is given by

$$\begin{aligned} \text{Replace } \frac{\partial u}{\partial t} & \text{ with } \frac{u_j^{n+1} - u_j^n}{\Delta t}. \\ \text{Replace } \frac{\partial u}{\partial x} & \text{ with } \frac{1}{2} \left( \frac{u_{j+1}^n - u_{j-1}^n}{2\Delta x} + \frac{u_{j+1}^{n+1} - u_{j-1}^{n+1}}{2\Delta x} \right). \end{aligned}$$

While these two implicit schemes are stable and therefore convergent for smooth data, they both work poorly for problems that have discontinuous solutions. This fact results from their large phase errors in the high frequencies. It is also possible to build an explicit conditionally stable centered scheme by the addition of artificial viscosity. A second order in space and time scheme for (1.1) is the popular Lax-Wendroff scheme

$$\begin{aligned} u_j^{n+1} = u_j^n & - \frac{\Delta t}{2\Delta x} \lambda (u_{j+1}^n - u_{j-1}^n) \\ & + \frac{1}{2} \left( \frac{\Delta t}{\Delta x} \lambda \right)^2 (u_{j+1}^n - 2u_j^n + u_{j-1}^n). \end{aligned}$$

This scheme also produces poor results when the solution to (1.1) is not smooth. To see this, consider (1.1) with  $\lambda = 1$  and with initial data

$$u(x, 0) = u_0(x) = \begin{cases} 1 & \text{if } |x - 1/2| \leq 0.10, \\ 0 & \text{otherwise} \end{cases},$$

(see the left pulse around  $x = 0.5$  in figure 1.1). The exact solution to this problem at  $t = 1.0$  is just the pulse translated to the right by 1 unit, (see the right pulse around  $x = 1.5$ ). The small boxes in figure 1.1 depict the numerical results to this problem coming from the Lax-Wendroff difference scheme.

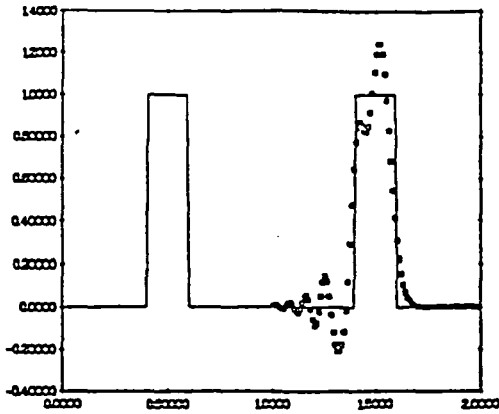


Figure 1.1. The solid line represents the initial data and exact solution at  $t = 1.0$ . The small boxes indicate the grid values coming from the Lax-Wendroff difference scheme.

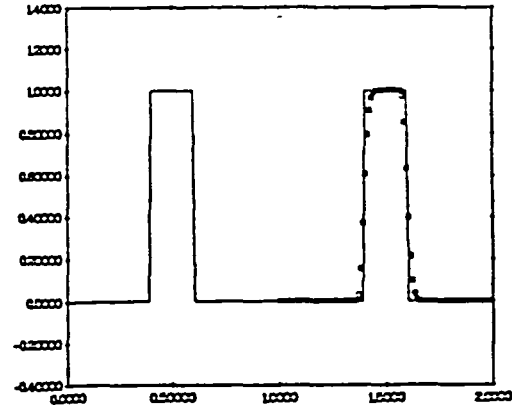


Figure 1.2. The solid line represents the initial data and exact solution at  $t = 1.0$ . The small boxes indicate the grid values coming from one of our modified fourth order central difference schemes.

The *wiggles* are a result of the high frequency phase error inherent to the Lax-Wendroff scheme.

When simulating the flow of air around hypersonic spacecraft on reentry, large gradient flows are the rule and not the exception. It should be obvious from the simple example above that traditional finite difference schemes can yield less than satisfactory results in these flow regimes. A certain amount of care must therefore be given to the design of numerical approximation techniques to accurately solve hypersonic flow problems. Eliminating nonphysical oscillations that are intrinsic to approximations coming from centered schemes applied to nonlinear systems of conservation laws is the main focus of this work. We modify a class of central space difference schemes to completely eliminate spurious numerical oscillations found in the example above. Compare the results coming from one of our modified central schemes presented in figure 1.2. Our modified schemes are intended to be simple enough so as to easily lend themselves to reliably approximate solutions to the equations governing the reentry of hypersonic spacecraft.

§2. The modified centered scheme for the scalar law. In this section, we develop a simple modification to a central differencing scheme applied to nonlinear, scalar, conservation laws of the form:

$$(2.1) \quad \frac{\partial}{\partial t} u + \frac{\partial}{\partial x} f(u) = 0.$$

An explicit forward Euler in time and central differencing in space finite difference formula applied to this problem is written as

$$(2.2) \quad u_j^{n+1} = u_j^n - \frac{\Delta t}{\Delta x} \left( f(u_{j+1/2}^n) - f(u_{j-1/2}^n) \right),$$

where  $u_j^n$  is used to indicate the approximation of  $u(x, t)$  at time level  $t^n$  and spatial grid block centered at  $x_j$ .  $u_{j+1/2}^n$  will be used here to denote some approximation to  $u(x_{j+1/2}, t^n)$ . For example, if we take

$$u_{j+1/2}^n = \frac{1}{2}(u_{j+1}^n + u_j^n),$$

then the resulting scheme is second order accurate in space and first order in time. One could hardly ask for a simpler approximation scheme to solve a partial differential equation. Unfortunately, as demonstrated above, this second order in space central differencing scheme is strictly unstable. To stabilize the central space differencing approach, we add a *parameter free* nonlinear artificial viscosity term to the right hand side of (2.2). This added viscosity term will have the property that in regions where the numerical approximation is not at a local extrema, the numerical viscosity term is identically zero.

Throughout this section, we make the following assumptions concerning the midpoints required by the forward Euler difference scheme (2.2):

- (2.3a) For each  $j$ , the midpoint  $u_{j+1/2}$  is given by a continuous function of grid values  $u_k$ ,  $k = j, j \pm 1, j \pm 2, \dots$
- (2.3b) For each  $j$ , the midpoint  $u_{j+1/2}$  is restricted to lie in the interval given by neighboring grid values  $u_j$  and  $u_{j+1}$ .

The minmod function is defined by

$$\text{minmod}(x, y) = \begin{cases} \min(|x|, |y|) \text{sign}(x) & \text{if } x \cdot y \leq 0 \\ 0 & \text{if } x \cdot y > 0 \end{cases},$$

and we shall use the notation  $\widehat{u}_{Lj}^n = u_{j-1/2}^n - u_j^n$  and  $\widehat{u}_{Rj}^n = u_{j+1/2}^n - u_j^n$ . At each point  $x_{j+1/2}$  midway between grid blocks, we consider left and right point values given by the formulae

$$(2.4) \quad \begin{aligned} v_{j+1/2}^l &= u_j^n + \text{minmod}(\widehat{u}_{Rj}^n, \rho \widehat{u}_{Lj}^n), \\ v_{j+1/2}^r &= u_{j+1}^n + \text{minmod}(\widehat{u}_{Lj+1}^n, \rho \widehat{u}_{Rj+1}^n), \end{aligned}$$

where  $\rho \geq 0$  is a finite parameter.

*Remark 1: If (2.4), with any fixed  $\rho > 1$ , is applied to a smooth function  $u(x)$  that has no local extreme points in the interval  $(x_{j-1/2}, x_{j+3/2})$ , then for  $\Delta x$  sufficiently small*

$$(2.5) \quad v_{j+1/2}^l = v_{j+1/2}^r = u_{j+1/2}^n.$$

(The parameter  $\rho$  does not depend in any way on the grid size.)

Our modified forward Euler centered scheme now reads

$$(2.6) \quad u_j^{n+1} = u_j^n - \frac{\Delta t}{\Delta x} (h_f(v_{j+1/2}^r, v_{j+1/2}^l) - h_f(v_{j-1/2}^r, v_{j-1/2}^l)),$$

where  $h_f(u_1, u_2)$  is any continuous 2 point monotone flux function that is consistent to  $f(u)$  in the sense that

$$h_f(u, u) = f(u);$$

see [4]. Referring back to (2.5), note that we should expect generically that

$$h_f(v_{j+1/2}^r, v_{j+1/2}^l) = f(u_{j+1/2}^n),$$

so we should expect that generically (2.6) will reduce to the centered scheme given in (2.2). The modified scheme can be written as

$$(2.7) \quad u_j^{n+1} = u_j^n - \frac{\Delta t}{\Delta x} (f(u_{j+1/2}^n) - f(u_{j-1/2}^n) - (Q_{j+1/2} - Q_{j-1/2})),$$

where

$$Q_{j+1/2} = f(u_{j+1/2}^n) - h_f(v_{j+1/2}^r, v_{j+1/2}^l),$$

so as to indicate the particular form of the modification to the centered scheme (2.2).

The modified forward Euler central difference scheme (2.6) satisfies in an obvious way the following theorem:

**THEOREM 1.** *Suppose all intermediate points  $u_{j+1/2}^n$  satisfy (2.3). Let  $\Delta t_h$  denote the time step stability limit for the first order monotone scheme*

$$u_j^{n+1} = u_j^n - \frac{\Delta t}{\Delta x} (h_f(u_{j+1}^n, u_j^n) - h_f(u_j^n, u_{j-1}^n)).$$

*If the time step size  $\Delta t$  in (2.6) is taken so that*

$$\Delta t \leq \frac{1}{\rho + 1} \Delta t_h,$$

*for the fixed  $1 \leq \rho < \infty$  in (2.4), then we have for each  $n > 0$*

$$\min_j u_j^0 \leq u_j^n \leq \max_j u_j^0.$$

*Moreover, if we use  $\text{Var}(u_j)$  to denote the usual pointwise variation of a grid values  $u_j$ , we have for each  $n > 0$*

$$\text{Var}(u_j^n) \leq \text{Var}(u_j^0).$$

**Remark 2:** *From the statement of Theorem 1, one should ask the following paradoxical question: Remark 1 seems to imply that if the solution to the pde that (2.6) approximates is smooth, then (2.6) reduces generically to the strictly unstable scheme (2.2). How can*

the claim of the theorem then be correct? This question will be addressed at the end of this section.

*Proof of Theorem 1:* In each cell  $I_j \equiv [x_{j-1/2}, x_{j+1/2})$  determine a number  $\theta_j$  such that

$$(1/2 + \theta_j)(v_{j-1/2}^r - u_j^n) + (1/2 - \theta_j)(v_{j+1/2}^l - u_j^n) = 0.$$

From the definitions of  $v_{j-1/2}^r$  and  $v_{j+1/2}^l$  we have for each  $j$

$$|\theta_j| \leq 1/2 \left| \frac{\rho - 1}{\rho + 1} \right|.$$

Cut  $I_j$  into two pieces with the dividing point given by  $\bar{x}_j = x_j + \theta_j \Delta x$ ; that is  $I_j = [x_{j-1/2}, \bar{x}_j) \cup [\bar{x}_j, x_{j+1/2}) \equiv I_j^l \cup I_j^r$ . Redistribute data  $u^n$  onto a nonuniform mesh given by  $\bigcup_j (I_j^l \cup I_j^r)$ , and let  $\bar{u}^n$  denote the redistributed data:

$$\bar{u}^n(x) = \begin{cases} v_{j-1/2}^r & \text{if } x \in I_j^l \\ v_{j+1/2}^l & \text{if } x \in I_j^r \end{cases}.$$

Scheme (2.6) amounts to nothing more than a classic monotone finite difference scheme applied to data  $\bar{u}^n$  on a nonuniform mesh, and reaveraged back onto the original mesh. Since the minimum grid spacing of the nonuniform mesh is

$$\frac{1}{\rho + 1} \Delta x,$$

the results in [4] make the results of the present theorem obvious.

The backward Euler version of (2.6) reads:

$$(2.8) \quad u_j^{n+1} = u_j^n - \frac{\Delta t}{\Delta x} (h_f(v_{j+1/2}^r, v_{j+1/2}^l) - h_f(v_{j-1/2}^r, v_{j-1/2}^l)),$$

where for the implicit scheme we define

$$\begin{aligned} \widehat{u}_{Lj}^{n+1} &= u_{j-1/2}^{n+1} - u_j^{n+1} \\ \widehat{u}_{Rj}^{n+1} &= u_{j+1/2}^{n+1} - u_j^{n+1} \end{aligned}$$

to get

$$\begin{aligned} v_{j+1/2}^l &= u_j^{n+1} + \min\text{mod}(\widehat{u}_{Rj}^{n+1}, \rho \widehat{u}_{Lj}^{n+1}), \\ v_{j+1/2}^r &= u_{j+1}^{n+1} + \min\text{mod}(\widehat{u}_{Lj+1}^{n+1}, \rho \widehat{u}_{Rj+1}^{n+1}). \end{aligned}$$

We assume that the midpoint values  $u_{j+1/2}^{n+1}$  are given by a continuous function of grid values at time level  $n + 1$ , and that they satisfy (2.3). Therefore, both  $v_{j+1/2}^l$  and  $v_{j+1/2}^r$  are continuous functions of grid values.

**THEOREM 2.** *The results of the previous theorem remain valid for the backward Euler scheme (2.8) without any CFL restrictions regardless of the size of  $1 \leq \rho < \infty$ .*

*Proof:* The idea here is quite simple. Consider a compact and convex subspace of the space of sequences defined by

$$\mathcal{D} = \{x : \text{Var}(x_j) \leq \text{Var}(u_j^n)\} \cap \{x : \min_j(u_j^n) \leq x_j \leq \max_j(u_j^n)\}.$$

Next, define

$$\begin{aligned} v_{j+1/2}^l(x) &= x_j + \min\text{mod}(\widehat{x}_{Rj}, \rho \widehat{x}_{Lj}), \\ v_{j+1/2}^r(x) &= x_{j+1} + \min\text{mod}(\widehat{x}_{Lj+1}, \rho \widehat{x}_{Rj+1}), \end{aligned}$$

and  $\Delta F_j(x)$  by

$$\Delta F_j(x) = h_f(v_{j+1/2}^r(x), v_{j+1/2}^l(x)) - h_f(v_{j-1/2}^r(x), v_{j-1/2}^l(x)).$$

We use

$$u_j^{n+1} = u_j^n - \frac{\Delta t}{\Delta x} \Delta F_j(u^{n+1}).$$

to denote the backward Euler scheme (2.8). We will show: (i) The implicit equation above has a solution. (ii) The solution obeys the stability results of Theorem 1. In order to accomplish these goals, consider the continuous map  $\mathcal{F}$  on  $\mathcal{D}$  defined by

$$\mathcal{F}_j(x) = x_j - \epsilon \left( x_j + \frac{\Delta t}{\Delta x} \Delta F_j(x) - u_j^n \right).$$

$\mathcal{F}$  can be rewritten as

$$\mathcal{F}_j(x) = (1 - \epsilon) \left( x_j - \frac{\epsilon}{1 - \epsilon} \frac{\Delta t}{\Delta x} \Delta F_j(x) \right) + \epsilon u_j^n.$$

From Theorem 1 it is clear that for  $\epsilon$  small enough

$$\begin{aligned} \text{Var}(\mathcal{F}_j(x)) &\leq (1 - \epsilon) \text{Var}(x_j) + \epsilon \text{Var}(u_j^n), \\ (1 - \epsilon) \min_j(x_j) + \epsilon \min_j(u_j^n) &\leq \mathcal{F}_j(x) \leq (1 - \epsilon) \max_j(x_j) + \epsilon \max_j(u_j^n). \end{aligned}$$

Therefore, we have that  $\mathcal{F} : \mathcal{D} \rightarrow \mathcal{D}$ . So by the Schauder fixed-point theorem [1], there exists a  $u^{n+1} \in \mathcal{D}$  such that  $u^{n+1} = \mathcal{F}(u^{n+1})$ , and the fixed-point  $u^{n+1}$  is a solution to the backward Euler scheme (2.8). Moreover, since  $u^{n+1} \in \mathcal{D}$  it also satisfies the desired stability properties.

A second order central differencing scheme is generated by the intermediate point value formula

$$(2.9) \quad u_{j+1/2} = \frac{1}{2}(u_{j+1} + u_j).$$



Clearly (2.9) satisfies conditions (2.3a) and (2.3b). We now derive a fourth order in space centered scheme. Let  $c_{j+1/2}(x)$  denote the cubic polynomial that interpolates the cell averages  $u_{j-1}$ ,  $u_j$ ,  $u_{j+1}$  and  $u_{j+2}$  on cells  $(x_{j-3/2}, x_{j-1/2})$ ,  $(x_{j-1/2}, x_{j+1/2})$ ,  $(x_{j+1/2}, x_{j+3/2})$  and  $(x_{j+3/2}, x_{j+5/2})$  respectively. If  $c_{j+1/2}(x)$  is applied to the values of a smooth function  $u(x, \cdot)$ , we have that  $c_{j+1/2}(x_{j+1/2}) = u(x_{j+1/2}, \cdot) + \epsilon(x_{j+1/2})$ , where  $\epsilon(x)$  depends smoothly on  $x$  and  $\epsilon(x) = O(\Delta x^4)$ . Therefore, since

$$\frac{1}{\Delta x} \int_{x_{j-1/2}}^{x_{j+1/2}} \frac{\partial}{\partial x} f(u(x, t)) dx = \frac{1}{\Delta x} (f(u(x_{j+1/2}, t)) - f(u(x_{j-1/2}, t))),$$

we have that this is equal to

$$\frac{1}{\Delta x} (f(c_{j+1/2}(x_{j+1/2})) - f(c_{j-1/2}(x_{j-1/2}))) + O(\Delta x^4).$$

The formula for  $c_{j+1/2}(x_{j+1/2})$  is

$$(2.10) \quad c_{j+1/2}(x_{j+1/2}) = \frac{1}{2}(q_l + q_r),$$

where,

$$\begin{aligned} q_l &= \frac{1}{2}(u_{j+1} + u_j) - \frac{1}{6}(u_{j+1} - 2u_j + u_{j-1}) \\ q_r &= \frac{1}{2}(u_{j+1} + u_j) - \frac{1}{6}(u_{j+2} - 2u_{j+1} + u_j), \end{aligned}$$

however,  $c_{j+1/2}(x_{j+1/2})$  does not always satisfy (2.3). Verification of (2.3) is crucial! We can ensure that (2.3) is satisfied by modifying  $q_l$  and/or  $q_r$  when necessary. We have taken the following approach: Let

$$\begin{aligned} (2.11) \quad \bar{q}_l &= \frac{1}{2}(u_{j+1} + u_j) \\ &\quad - \frac{1}{6} \min(|u_{j+1} - 2u_j + u_{j-1}|, 3|u_{j+1} - u_j|) \text{sign}(u_{j+1} - 2u_j + u_{j-1}), \\ \bar{q}_r &= \frac{1}{2}(u_{j+1} + u_j) \\ &\quad - \frac{1}{6} \min(|u_{j+2} - 2u_{j+1} + u_j|, 3|u_{j+1} - u_j|) \text{sign}(u_{j+2} - 2u_{j+1} + u_j), \end{aligned}$$

and note that  $\bar{q}_l$  and  $\bar{q}_r$  verify (2.3). So we define

$$(2.12) \quad u_{j+1/2} \equiv \frac{1}{2}(\bar{q}_l + \bar{q}_r)$$

and note that (2.12) satisfies (2.3) as well. However, when (2.12) is applied to a smooth function away from local extrema, we have that for sufficiently small  $\Delta x$

$$u_{j+1/2} \equiv \frac{1}{2}(q_l + q_r) = c_{j+1/2}(x_{j+1/2}),$$

therefore giving the desired accuracy away from extreme points of the solution.

We conclude this section by addressing Remark 2. Consider the linear pde with 1-periodic boundary conditions

$$(2.13) \quad \begin{aligned} \frac{\partial}{\partial t} u + \frac{\partial}{\partial x} u &= 0 \\ u(0, t) &= u(1, t) \\ u(x, 0) &= \sin(2\pi x). \end{aligned}$$

To approximate the solution to this pde, we will use the following fourth order in space, forward Euler scheme:

$$(2.14) \quad u_j^{n+1} = u_j^n - \frac{\Delta t}{\Delta x} (v_{j+1/2}^l - v_{j-1/2}^l),$$

where

$$\begin{aligned} v_{j+1/2}^l &= u_j^n + \min\text{mod}(\widehat{u}_{Rj}^n, \rho \widehat{u}_{Lj}^n) \\ \widehat{u}_{Lj}^n &= u_{j-1/2}^n - u_j^n \quad \widehat{u}_{Rj}^n = u_{j+1/2}^n - u_j^n \\ u_{j+1/2}^n &= \frac{1}{2}(\bar{q}_l + \bar{q}_r), \quad \text{see (2.11)}. \end{aligned}$$

Notice that at grid points where the approximate solution generated by (2.14) is not near a local extremum, we have that

$$v_{j+1/2}^l = \frac{1}{2}(q_l + q_r), \quad \text{see (2.10),}$$

and one can easily verify that (2.14), using these point values, is strictly unstable – for every nontrivial Fourier mode. However, the results of Theorem 1 imply that the approximate solution generated by the full nonlinear scheme (2.14) is stable. What in fact happens is the following: The scheme away from extrema is unstable and all Fourier modes are geometrically amplified. When an oscillation begins to form, the nonlinear *limiting* mechanism kicks in where local extreme points appear. This limiting will tend to flatten out extreme points producing a *staircase* effect. This phenomena is demonstrated using (2.14) to approximate the solution to (2.13) using  $\Delta x = 1/100$  and the results are plotted in figure 2.1 at  $t = 1.0$

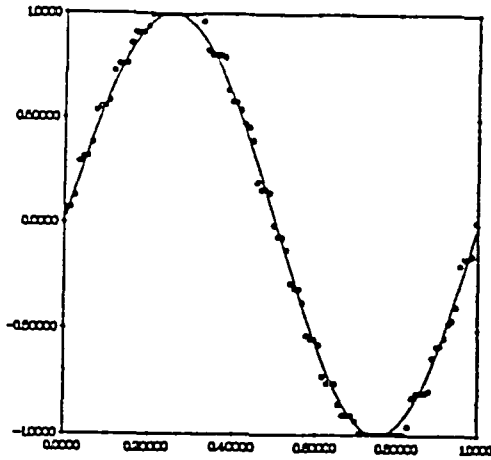


Figure 2.1. The solid line represents the exact solution to (2.13) at  $t = 1.0$ . The circles depict the approximate solution coming from (2.14).

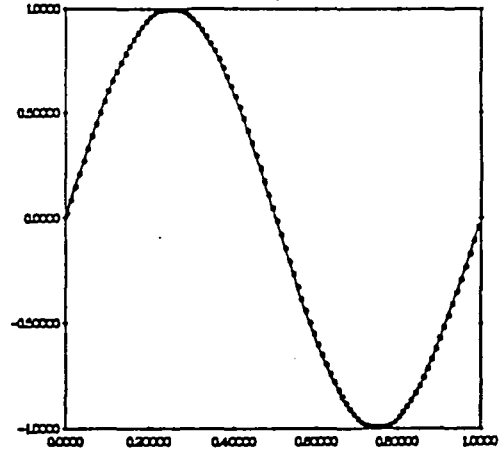


Figure 2.2. The solid line represents the exact solution to (2.13) at  $t = 1.0$ . The circles depict the approximate solution coming from (2.15).

While the results above do not contradict the results from Theorem 1, they should however be considered unsatisfactory. To eliminate this staircase phenomena, (this phenomena is inherent to our modified forward Euler central schemes), we introduce a Lax-Wendroff type of viscosity to the right hand side of (2.14). Specifically, we modify (2.14) to

$$(2.15) \quad u_j^{n+1} = u_j^n - \frac{\Delta t}{\Delta x} ((v_{j+1/2}^l - S_{j+1/2}) - (v_{j-1/2}^l - S_{j-1/2})),$$

where

$$S_{j+1/2} = \frac{1}{2} \left( \frac{\Delta t}{\Delta x} \right) \frac{v_{j+1/2}^l - u_j^n}{u_j^n - v_{j-1/2}^r} (v_{j+1/2}^l - v_{j-1/2}^r).$$

This modification leads to a scheme that is generically fourth order in space and *second* order in time. More importantly however, in regions where the solution to the pde is smooth, (2.15) reduces to a stable numerical scheme. The results from (2.15) are plotted in figure 2.2. Implicit schemes of the form (2.8) do not exhibit the staircase phenomena demonstrated above for explicit schemes. The viscosity modification hinted to above in (2.15) will be analyzed and generalized in future work.

**§3. Hyperbolic systems and numerical examples.** The extension of the implicit scheme (2.8) to hyperbolic systems is straight-forward. Numerical results coming from the implicit scheme applied to hypersonic reentry problems will appear in a future paper with C. P. Li of NASA Johnson Space Center. The extension of the modified explicit scheme (2.6) to time dependent hyperbolic systems is not so straight-forward. As demonstrated in the examples depicted in figures 2.1 and 2.2, some type of numerical viscosity must be appended to the basic central scheme. At present, we take the approach outlined below.

Consider a one space dimensional, hyperbolic system of  $m$  equations

$$(3.1) \quad \begin{aligned} \frac{\partial}{\partial t} u + \frac{\partial}{\partial x} f(u) &= 0, \\ u \in \mathbb{R}^m, \quad f : \mathbb{R}^m &\rightarrow \mathbb{R}^m, \end{aligned}$$

and let  $Df(u)$  denote the Jacobian matrix of  $f(u)$ . Since (3.1) is hyperbolic, the matrix  $Df(u)$  has  $m$  real eigenvalues, denoted here by  $\lambda_k(u)$ ,  $k = 1, \dots, m$  and  $m$  independent eigenvectors, denoted here by  $r_k(u)$ ,  $k = 1, \dots, m$ . We let  $R(u)$  denote the matrix whose columns are the right eigenvectors of  $Df(u)$ ,

$$R(u) = (r_1(u) \quad \cdots \quad r_m(u)),$$

and

$$L(u) = R^{-1}(u).$$

The domain and range of the minmod function is extended to  $\mathbb{R}^m$  component-wise. That is, for each  $1 \leq i \leq m$

$$(\text{minmod}(\vec{x}, \vec{y}))_i = \text{minmod}(x_i, y_i).$$

The modification of (2.4) to systems is to perform the limiting in so-called *characteristic variables*. Written in matrix form, this procedure is given by

$$(3.2) \quad \begin{aligned} \vec{v}_{j+1/2}^l &= \vec{u}_j^n + R(u_j^n) \text{minmod}(L(u_j^n) \widehat{u}_{Rj}^n, \rho L(u_j^n) \widehat{u}_{Lj}^n), \\ \vec{v}_{j+1/2}^r &= \vec{u}_{j+1}^n + R(u_{j+1}^n) \text{minmod}(L(u_{j+1}^n) \widehat{u}_{Lj+1}^n, \rho L(u_{j+1}^n) \widehat{u}_{Rj+1}^n), \end{aligned}$$

The simplest numerical flux  $h_f(u_1, u_2)$  we can envision (see (2.6)) is the Lax-Friedrichs numerical flux function. It is given by

$$(3.3) \quad h_f^{LF}(u_1, u_2) = \frac{1}{2} ((f(u_1) + f(u_2)) - \nu(u_1 - u_2)),$$

where the parameter  $\nu$  is an artificial viscosity satisfying

$$\nu \geq \max_k (\max(|\lambda_k(u_1)|, |\lambda_k(u_2)|)).$$

Since generically we will have that  $u_1 = u_2$ , the Lax-Friedrichs viscosity term above will vanish so that generically we will have that

$$h_f^{LF}(u_1, u_2) = f(u_1) = f(u_2).$$

Finally, the viscosity modification used in (2.15) will be extended to nonlinear systems of equations in the following way. Define  $\widehat{c}_{Lj}$  and  $\widehat{c}_{Rj}$  by

$$(3.4) \quad \widehat{c}_{Lj} = \text{minmod}(L(u_j^n) \widehat{u}_{Lj}^n, \rho L(u_j^n) \widehat{u}_{Rj}^n),$$

$$\widehat{c}_{Rj} = \text{minmod}(L(u_j^n)\widehat{u}_{Rj}^n, \rho L(u_j^n)\widehat{u}_{Lj}^n),$$

and from these define

$$\begin{aligned} s_{Lj} &= -(\widehat{c}_{Rj} - \widehat{c}_{Lj}) (\widehat{c}_{Lj}/\widehat{c}_{Rj}), \\ s_{Rj} &= -(\widehat{c}_{Rj} - \widehat{c}_{Lj}) (\widehat{c}_{Rj}/\widehat{c}_{Lj}), \end{aligned}$$

Note that both  $s_{Lj}$  and  $s_{Rj}$  are well defined and continuous functions of  $\widehat{u}_{Lj}^n$  and  $\widehat{u}_{Rj}^n$ . Now in each cell  $j$  and for each vector component  $k$ , compute

$$\begin{aligned} (3.5) \quad (d_{Lj})_k &= 1/2 \frac{\Delta t}{\Delta x} \min(\lambda_k(u_j), 0)^2 (s_{Lj})_k, \\ (d_{Rj})_k &= 1/2 \frac{\Delta t}{\Delta x} \max(\lambda_k(u_j), 0)^2 (s_{Rj})_k. \end{aligned}$$

The full numerical flux function we use in our forward Euler calculations below is given by

$$(3.6) \quad h_{fj+1/2} = h_f^{LF}(\bar{v}_{j+1/2}^r, \bar{v}_{j+1/2}^l) - (R(u_{j+1}^n)d_{Lj+1} + R(u_j^n)d_{Rj}),$$

giving the scheme

$$u_j^{n+1} = u_j^n - \frac{\Delta t}{\Delta x} (h_{fj+1/2} - h_{fj-1/2}).$$

We consider the fourth order modified central scheme (3.6) taking the limit factor  $\rho = 3.0$  and using a Courant number  $CFL = 0.25$ . This scheme is applied to the one dimensional Euler equations

$$\begin{aligned} \frac{\partial}{\partial t} \rho + \frac{\partial}{\partial x} \rho u &= 0, \\ \frac{\partial}{\partial t} \rho u + \frac{\partial}{\partial x} (\rho u^2 + p) &= 0, \\ \frac{\partial}{\partial t} e + \frac{\partial}{\partial x} (e + p)u &= 0. \end{aligned}$$

In the equations above,  $\rho$  is a fluid's density,  $u$  its velocity and  $e$  its total energy. The pressure  $p$  is given by the equation of state  $p = (\gamma - 1)(e - \rho u^2)$  where the parameter  $\gamma = 1.4$ . The Riemann problem initial datum

$$(\rho(x), u(x), p(x)) = \begin{cases} (.445, .698, 3.528) & \text{if } x < 0.5 \\ (.5, 0, .571) & \text{if } x \geq 0.5 \end{cases},$$

defines what is frequently referred to as the Lax Riemann problem. This datum is integrated to time  $t = 0.15$ . See [7,2,6] for comparisons. 100 equally spaced points on the interval  $(0, 1)$  are used for all results presented here. In all figures below, the solid lines represent the exact fluid density and the  $x$ 's denote its numerical approximation.

Figure 3.1 depicts the results of the second order Lax-Wendroff finite difference scheme applied to the Lax Riemann test problem above with  $CFL = 0.8$ . Figure 3.2 depicts the results of the first order Lax-Friedrichs finite difference scheme applied to this same test problem. Figure 3.3 depicts our new scheme (3.6) applied to the Lax test problem.

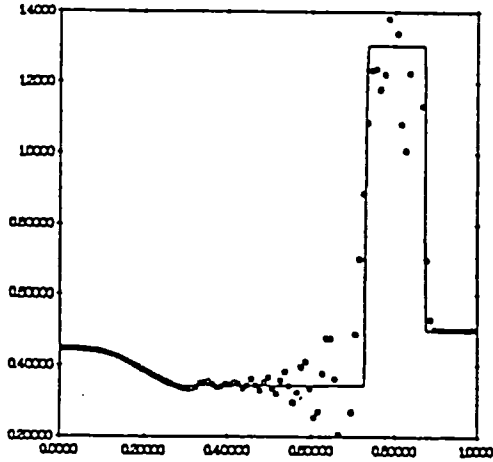


Figure 3.1. The solid line represents the exact solution to the Lax Riemann problem. The  $x$ 's are results from the Lax-Wendroff scheme.

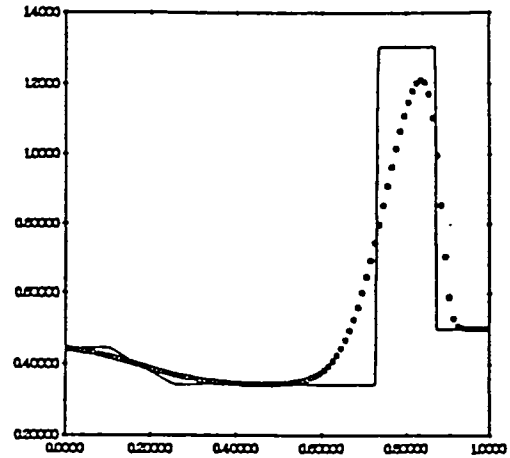


Figure 3.2. Results coming from the Lax-Friedrichs scheme.

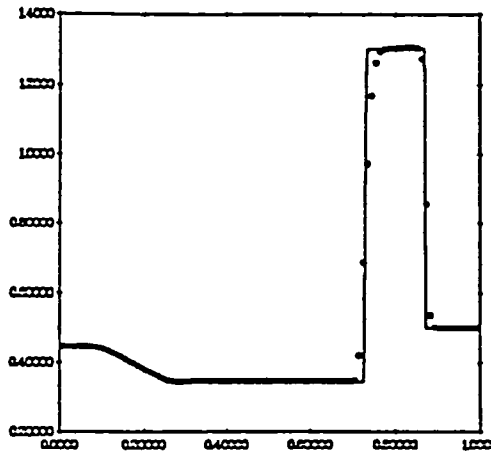


Figure 3.3. Numerical results coming from our fourth order scheme (3.6).

The next test problem is referred to as the *blast wave* problem. This problem tests the performance of a numerical scheme on very strong shocks and shock wave interactions.

Its initial data contains two shock waves with pressure ratios of 100,000 and 10,000. The initial data to this problem is

$$(\rho(x), u(x), p(x)) = \begin{cases} (1.0, 0.0, 1000.0) & \text{if } x < 0.1 \\ (1.0, 0.0, 0.01) & \text{if } 0.1 \leq x \leq 0.9, \\ (1.0, 0.0, 100.0) & \text{if } x > 0.9 \end{cases}$$

The boundary conditions at  $x = 0$  and  $x = 1$  are reflecting. The Lax-Wendroff scheme will not solve this problem. The initial shocks are so strong that negative densities and pressures occur almost immediately. The Lax-Friedrichs scheme will solve it – be it not very well. Figure 3.4 depicts the Lax-Friedrichs results using 400 points comparing it to the “exact” solution which came from (3.6) using 1200 points. (The exact solution to this problem can not be found in closed form.) Figure 3.5 demonstrates the performance of our scheme (3.6) on the blast wave test problem again using 400 points. We should point out that no modifications of the scheme was required to avoid negative densities and pressures.

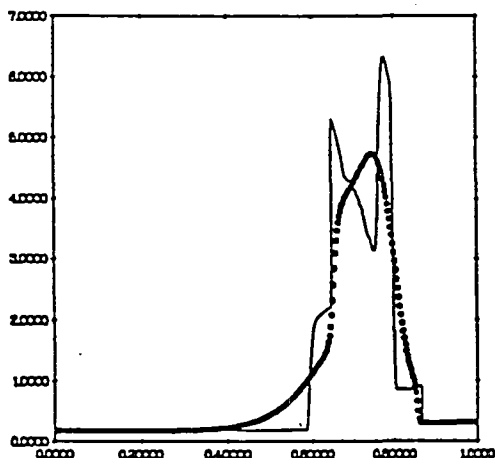


Figure 3.4. The Lax-Friedrichs scheme applied to the blast wave test problem.

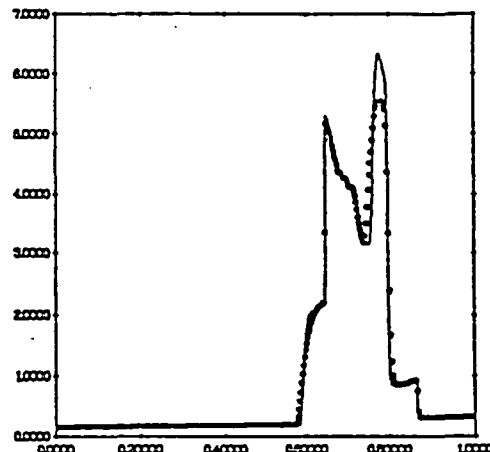


Figure 3.5. Results coming from scheme (3.6).

#### REFERENCES

- [1] N. Dunford and J.T. Schwartz, *Linear Operators, Part I: General Theory*, Pure and Appl. Math., vol VII, Interscience, New York, 1958.
- [2] A. Harten and S. Osher, “Uniformly high-order accurate nonoscillatory schemes. I”, *SIAM J. Numer. Anal.* 24 (1987), pp. 279-309.
- [3] P. D. Lax, “Weak solutions of nonlinear hyperbolic equations and their numerical computation”, *Comm. Pure Appl. Math.* 7, pp. 159-193.
- [4] R. Sanders, “On convergence of monotone finite difference schemes with variable spatial differencing”, *Math. Comp.* 40 (1983) pp. 91-106.

- [5] R. Sanders, "A third order accurate variation nonexpansive difference scheme for single nonlinear conservation laws", *Math. Comp.* 51 (1988) pp. 535-558.
- [6] R. Sanders and A. Weiser, "A high order staggered grid method for hyperbolic systems of conservation laws in one space dimension", *Computer Methods in Applied Mechanics and Engineering.* 75 (1989) pp. 91-107.
- [7] G.A. Sod, "A survey of several finite difference methods for systems of nonlinear hyperbolic conservation laws", *J. Comp. Phys.* 27 (1978), pp. 1-31.